

A11102 461545

NAT'L INST OF STANDARDS & TECH R.I.C.



A11102461545

Cooper, Leonard Y/Ceiling jet properties
QC100 .U56 NO.86-3307 V1986 C.1 NBS-PUB-

Reference

NBSIR 86-3307

NBS

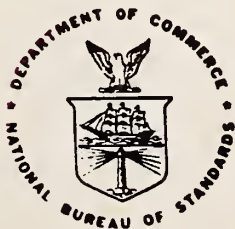
PUBLICATIONS

Ceiling Jet Properties and Wall Heat Transfer in Compartment Fires Near Regions of Ceiling Jet-Wall Impingement

Leonard Y. Cooper

U.S. DEPARTMENT OF COMMERCE
National Bureau of Standards
National Engineering Laboratory
Center for Fire Research
Gaithersburg, MD 20899

January 1986



U.S. DEPARTMENT OF COMMERCE
NATIONAL BUREAU OF STANDARDS

QC

100

.U56

86-3307

1986

QC
100
436
86-3307
1986

NBSIR 86-3307

600
**CEILING JET PROPERTIES AND WALL
HEAT TRANSFER IN COMPARTMENT
FIRES NEAR REGIONS OF CEILING
JET-WALL IMPINGEMENT**

Leonard Y. Cooper

U.S. DEPARTMENT OF COMMERCE
National Bureau of Standards
National Engineering Laboratory
Center for Fire Research
Gaithersburg, MD 20899

January 1986

U.S. DEPARTMENT OF COMMERCE, Malcolm Baldrige, *Secretary*
NATIONAL BUREAU OF STANDARDS, Ernest Ambler, *Director*

TABLE OF CONTENTS

	Page
LIST OF FIGURES	iv
Abstract	1
1. INTRODUCTION	2
2. THE BASIC PHENOMENA	2
3. CEILING JET-WALL IMPINGEMENT	4
4. HEAT TRANSFER FROM IMPINGING TWO-DIMENSIONAL PLANE AIR JETS	6
5. EQUIVALENCE BETWEEN THE PLANE JET AND THE CEILING JET AT THE IMPINGEMENT POINT	8
6. STAGNATION POINT HEAT TRANSFER	10
7. COMPARISON WITH EXPERIMENTAL DATA	12
8. OTHER USEFUL PROPERTIES OF THE CEILING JET	12
9. AN ESTIMATE OF THE RANGE OF UTILITY OF THE RESULTS	15
10. REFERENCES	17
11. NOMENCLATURE	19

LIST OF FIGURES

	Page
Figure 1. Early time ceiling jet-wall interaction	22
Figure 2. Ceiling jet-wall interaction with upper layer:	
a) penetration of interface; b) no penetration of interface.....	23
Figure 3. Plane jet-wall impingement	24
Figure 4. A plot of stagnation line Nusselt number from Figure 2	
of [10] and from Eq. (4)	25
Figure 5. Stagnation point heat transfer amplification from Eq.(9):	
— "typical" full-scale; --- reduced scale	26
Figure 6. A plot of the integral I defined in Eq. (28)	27
Figure 7. A plot of $Q_{loss}/[(1-\lambda_r)Q]$ per Eqs. (27) and (32)	28

CEILING JET PROPERTIES AND WALL HEAT TRANSFER IN COMPARTMENT FIRES NEAR REGIONS OF CEILING JET-WALL IMPINGEMENT

Leonard Y. Cooper

Abstract

The problem of heat transfer to walls from fire plume-driven ceiling jets during compartment fires is introduced. An analogy is drawn between the flow dynamics and heat transfer at ceiling jet-wall impingement and at the line impingement of a wall and a two-dimensional, plane, free jet. Using the analogy, the literature on plane, free jet flows and corresponding wall stagnation heat transfer rates leads to readily useable estimates for the heat transfer from, and the mass, momentum, and enthalpy fluxes of the turned compartment fire ceiling jet as it begins its initial descent as a negatively buoyant flow along the compartment walls. Available data from a reduced-scale experiment provides some limited verification of the heat transfer estimate. Depending on the proximity of a wall to the point of plume-ceiling impingement, the estimates indicate that for "typical" full-scale compartment fires with energy release rates in the range 200-2000kW and fire-to-ceiling distances of 2-3m, the rate of heat transfer to walls can be enhanced by a factor of 1-2.5 over the heat transfer to ceilings immediately upstream of ceiling jet-wall impingement.

1. INTRODUCTION

In potentially hazardous compartment fires, the total heat transfer from fire plume-driven ceiling and wall flows to enclosure ceiling and wall surfaces can be a significant fraction of the fire's total energy release rate, Q . [1, 2] This is especially true during the critical early times of such fires when events which relate strongly to the ultimate safety of people and property are taking place, e.g., during times of significant fire detector and/or sprinkler link response; when fire compartment environments hazardous to people are developing, and up to times when they are approached; up to the time when temperatures of combustible ceiling and wall surfaces reach ignition temperatures, and when they are relatively low compared to characteristic temperatures of the fire plume. Successful simulations of such critical events must involve reasonably accurate mathematical models of the above-mentioned heat transfer and related flow phenomena.

Algorithms to estimate heat transfer to smooth ceilings during compartment fires, which are concise enough to code into subroutines for use in practical zone-type compartment fire model computer codes, are now available [1, 3-5]. Such is not the case for the potentially significant heat transfer to the compartment walls. It is the purpose of this paper to develop a means of estimating the heat transfer from ceiling jet driven wall flows to wall surfaces. Another goal of this work is to develop estimates for those properties of ceiling jets, immediately upstream of wall impingement, which are required to predict the characteristics of ensuing downward, negatively buoyant wall flows.

2. THE BASIC PHENOMENA

As a fire grows in an enclosure, the elevated temperature air and products of combustion which leave the zone of the burning object form a plume and are convected upward by buoyancy. When the upward movement of the plume constituents are blocked by the ceiling (a distance, H , above the fire) they spread

radially outward forming a relatively thin turbulent ceiling jet. Depending on the proximity, D , of vertical surfaces, this ceiling jet either loses most of its momentum far out on its trajectory (in the case of an expansive ceiling with large D/H surfaces), or can be expected to interact vigorously with these bounding surfaces (in the case of lower aspect ratio spaces with D/H of the order of 1) by forming a downward wall jet flow which is eventually turned back upward by its own buoyancy. The flow scenario for the latter case is depicted in Figure 1.

Once the ceiling jet gases are blocked by bounding vertical surfaces, they begin to redistribute themselves across the entire ceiling area of the enclosure. Eventually a relatively quiescent, stably stratified, upper gas layer is formed below the continuing ceiling jet activity. The bottom of this layer is defined by a distinctive material interface which separates the lower ambient air from the upper, heated, product of combustion-contaminated gases. With increased time the level of the interface continues to drop and the average absolute temperature, T_{up} , of the upper layer gases continues to rise. As depicted in Figure 2, for small to moderate D/H , vigorous ceiling jet-wall flow interaction can still occur. Two cases can be distinguished. In the first, depicted in Figure 2a, the downward wall jet penetrates the interface, continues its downward flow in the lower layer, and is eventually buoyed back upward to interact with the upper layer. In the second, depicted in Figure 2b, the downward flowing wall jet loses its downward momentum, and is turned back upward prior to penetrating the two-layer interface.

An experimental program to isolate and study the type of wall flows depicted in Figures 1 and 2 is in progress, and the first stage of this, which provides results for the flows of Figure 1 and 2b, has been completed [6]. To use the results of [6] and anticipated future results on wall flows requires an understanding, not now available, of the ceiling jet turning region near ceiling jet-wall impingement. It is the objective of the present work to begin to develop such an understanding.

The ceiling jet flow and heat transfer phenomena of Figure 2, which take place in the relatively

quiescent background environment of temperature T_{up} , are similar to those of Figure 1. Following ideas of [3], where the upper layer is treated as an expansive environment with ambient temperature T_{up} , quantitative descriptions of the latter phenomena would also be useable in predicting the former. For this reason it is sufficient to focus attention here on the relatively simple Figure 1 configuration.

3. CEILING JET-WALL IMPINGEMENT

The goal of the present analysis is to develop estimates for ceiling jet properties and for the heat transfer to the wall of Figure 1 near the ceiling-wall line of intersection, and where the radius vector, r , is normal to the wall.

It is known that for small to moderate values of r/H inertial forces are generally large compared to buoyancy forces (i.e., characteristic Richardson numbers, Ri , are small) in buoyant plume-driven ceiling jets [7]. This fact was used in [4] to argue that the flow and heat transfer characteristics of the buoyant plume-driven ceiling jets depicted in Figures 1-2 could be directly related to the analogous characteristics of wall or ceiling jets driven by heated or unheated free turbulent jets (i.e., flows with the same configurations of Figure 1, but with a turbulent jet replacing the fire and its buoyant plume). Presumably, a ceiling jet driven by a plume would have approximately identical flow properties as that driven by an equivalent free jet, at least up to r/H of the order of 1. The criteria of equivalence proposed in [4] was that the mass and momentum of the plume and of the free jet be identical at their respective points of impingement. Applying these criteria, it has been possible to recorelate results from the literature on free jet-driven wall flows, to use them with results from buoyant plume-driven ceiling jet experiments, and to obtain estimates for the ceiling jet flow and heat transfer characteristics of interest in compartment fires [1, 3-5].

Using the above ideas permits estimates for ceiling jet characteristics up to the point of wall

impingement. For example, upstream of this wall impingement point and outside of the ceiling impingement stagnation zone defined by $r/H < 0.2$, results of [8] indicate that the radial velocity distribution $V(Z)$, is essentially self-similar, and rises very rapidly from zero at the ceiling to a maximum, V_{\max} , at a distance $Z=0.23\delta$, δ being the distance below the ceiling where $V/V_{\max}=1/2$. Also, $V(Z/\delta=1.6)/V_{\max} \approx 0.2$. Finally, at any given radial position, and for $Z/\delta > 0.23$, results of reference [9] suggest that the V/V_{\max} profile can be approximated by the velocity profile of half of a plane, two-dimensional, free turbulent jet as depicted in Figure 3.

Define M_0' as the momentum flux of the ceiling jet per unit width (assumed to be of near-constant density, ρ , in the sense of the Boussinesq approximation)

$$M_0' = \rho V_{\max}^2 \delta \int_0^{\infty} (V/V_{\max})^2 d(Z/\delta) \quad (1)$$

As will be seen, an estimate of M_0' immediately upstream of ceiling jet-wall impingement will lead to a determination of the desired wall heat transfer at this location.

Based on the above-mentioned characteristics of the V/V_{\max} profile, it is assumed that the inner layer of the ceiling jet, i.e., from $Z/\delta=0$ to 0.23 , is thin in the sense that the integral of Eq.(1) between $0 < Z/\delta < 0.23$ is expected to be a small fraction of M_0' . This together with the noted similarity between the radially symmetric ceiling jet and half of the plane free jet suggests that the interaction of these two flows with vertical surfaces in Figure 1 and 3 configurations, respectively, would be approximately reproduced

If appropriate criteria of equivalence between the two upstream flows were satisfied. Note that in the case of the ceiling jet, the no-slip condition at the ceiling will lead to stagnation corner flows which are significantly different than the flows in the immediate vicinity of plane jet-wall stagnation. However, these corner flows will likely be confined to a relatively small region with characteristic dimension 0.23δ , and, with regard to wall heat transfer, it is reasonable to expect that they will have an effect primarily on a similarly small uppermost segment of the wall. Stagnation heat transfer results to be developed here are for the upper part of the wall which excludes such a segment.

4. HEAT TRANSFER FROM IMPINGING TWO-DIMENSIONAL PLANE AIR JETS

Reference [10] presents data from an experimental study of heat transfer from an ambient temperature plane jet to an isothermal wall (temperature, T_w) in a Figure 3-type configuration. For $X_n/B \geq 1.4$ and Reynold's number $Re_e > 2000$, a correlation for the stagnation point heat transfer coefficient, h_s , was found to be

$$Nu_0 = h_s B / k = 1.2 Re_e^{0.56} (X_n/B)^{-0.62} ; \quad Re_e = \rho u_e B / \mu \quad (2)$$

where X_n is the distance from the jet nozzle of width B , u_e is the uniform nozzle exit velocity, μ and k are the gas viscosity and thermal conductivity, respectively, and h_s is based on the temperature difference $(T_{amb} - T_w)$. Motivated by the expectation that for limiting large X_n/B (i.e., fully developed jets) h_s should depend explicitly on the characteristic length X , the distance from the virtual origin of the jet, and not on X_n or B , the data presented in [10] were reanalyzed. Based on a review of the literature in [11], X was taken to be

$$X = X_n + 1.95 B \quad (3)$$

The result was the following new correlation

$$\lim_{X/D \rightarrow \infty} Nu_s = 1.74 Re_s^{0.58} \quad (4)$$

$$Nu_s = h_s X / k = (X/B) Nu_0, \quad Re_s = (2M_0' \rho X)^{1/2} / \mu = (X/B)^{1/2} Re_e$$

where $2M_0'$ is the conserved momentum flux per unit width of the jet (e.g., $2M_0' = \rho B u_e^2$), and h_s is the stagnation point heat transfer coefficient based on the $(T_{amb} - T_w)$ temperature difference. The Figure 2 data correlation plots of [10] are reproduced here in Figure 4 along with the approximation of Eq. (4). For $Re_e \geq 2750$ and $X_n/B \geq 15$, Eq. (4) estimates all h_s data in the figure to within approximately five percent.

It is of interest here to extend the results of [10] in order to estimate heat transfer rates, q , from elevated temperature jets to nonuniform temperature walls. In a manner analogous to analyses in [1,3-5,12-13] the adiabatic wall temperature, T_{ad} , is introduced as a characteristic temperature, and it is assumed that an estimate for q can be obtained from

$$q = h(T_{ad} - T_w) \quad (5)$$

where T_w would generally vary with position from the stagnation point. Here, T_{ad} is the temperature

distribution adjacent to an adiabatic wall on which a plane jet from an elevated temperature source is impinging. $T_{ad} = T_{amb}$ in [10], and for this reason the assumed formulation of Eq.(5) is equivalent to the assumption that its h is identical to the h obtained in [10]. This is of particular interest here near the stagnation point where $h = h_s$.

5. EQUIVALENCE BETWEEN THE PLANE JET AND THE CEILING JET AT THE IMPINGEMENT POINT

In the Figure 3 configuration, h_s can be estimated by using the plane jet's impingement point values X and M_o' in Eq.(4). These will be chosen in a manner that would simulate the Figure 1 ceiling jet flow immediately upstream of the $r=D$ wall impingement point.

Reference [14] proposes the following for the plane jet velocity distribution

$$V/V_{max} = \exp[-\alpha(Z/X)^2] ; V_{max} = \beta[2M_o' / (\rho X)]^{1/2} \quad (6)$$

where conservation of momentum along the X axis requires

$$\beta^2 = (2\alpha/\pi)^{1/2} \quad (7)$$

Taking α in Eq.(6) to be the average of the two values, 75.0 and 70.7, found for the two experiments of [14], and using this in Eq.(7) leads to

$$\alpha = 72.8, \quad \beta = 2.61 \quad (8)$$

where the above value for β compares favorably with values of β which are consistent with three other plane jet models reviewed in [11], viz., $\beta = 2.56, 2.45$ and 2.83 .

As in Eq.(6) for the plane jet, for the purpose of estimating impingement wall heat transfer it is now assumed that the ceiling jet velocity immediately upstream of $r=D$ can also be simulated by a Gaussian distribution in Z . Then, immediately upstream of their respective impingement points, the flow distribution of the plane jet and ceiling jet would be equivalent if

$$Z_{\text{plane jet at } V=V_{\max}/2} = Z_{\text{ceiling jet at } V=V_{\max}/2} = \delta \quad (9)$$

$$V_{\max} \text{ of plane jet} = V_{\max} \text{ of ceiling jet} = V_{\max} \quad (10)$$

For plume-driven ceiling jets, results from [4] and [8] lead to

$$V_{\max}/V = 0.85(D/H)^{-1.1} \quad (11)$$

$$\delta/H = 0.10(D/H)^{0.9} \quad (12)$$

$$V = g^{1/2} H^{1/2} Q^{*1/3}, \quad Q^* = (1 - \lambda_r)Q / (\rho C_p T_{\text{amb}} g^{1/2} H^{5/2})$$

where g is the acceleration of gravity, C_p is the specific heat and λ_r is the fraction of Q radiated from the fire's combustion zone.

Using Eq.(12) and the first of Eqs. (6) in Eq.(9), and Eq. (11) and the second of Eqs. (6) in Eq.(10)

leads to the following respective properties of the equivalent plane jet

$$x/H = 1.0(D/H)^{0.9} \quad (13)$$

$$M_o' / (\rho H V^2) = 0.053(D/H)^{-1.3} \quad (14)$$

6. STAGNATION POINT HEAT TRANSFER

Eqs. (13) and (14) in Eqs. (4) yield the following relationship for h_s in terms of compartment fire parameters

$$h_s/h = 0.89 Re_H^{-0.42} Pr^{-1} (D/H)^{-1.02} \quad (15)$$

$$h = \rho C_p g^{1/2} H^{1/2} Q^{*1/3}; \quad Re_H = \rho g^{1/2} H^{3/2} Q^{*1/3} / \mu$$

where h and Re_H are a normalizing heat transfer coefficient and the characteristic impingement point Reynold's number, respectively, and where Pr is the Prandtl number.

To use Eq. (15) in Eq. (5) requires T_{ad} . This would be identical to $T_{ad}(r=D)$ for the ceiling jet [5]

$$\frac{[T_{ad}(r/H) - T_{amb}]}{T_{amb} Q^{*2/3}} = f(r/H) = \begin{cases} 10.22 - 14.9 r/H, & 0 \leq r/H \leq 0.2; \\ \frac{8.39 [1 - 1.10(r/H)^{0.8} + 0.808(r/H)^{1.6}]}{[1 - 1.10(r/H)^{0.8} + 2.20(r/H)^{1.6} + 0.690(r/H)^{2.4}]}, & r/H > 0.2 \end{cases} \quad (16)$$

Assuming identical wall and ceiling temperatures near the ceiling-wall junction, it is of interest to compare $q=q_s$ to the wall at the stagnation point to q_{ceiling} , the heat transfer rate to the ceiling, immediately upstream of the stagnation point. This would provide insight into the expected level of any heat transfer enhancement due to stagnation point flow conditions. Using Eq.(5) for both wall and ceiling, Eq.(6) of [5] for h_{ceiling} and Eq.(15), and taking $Pr=0.7$ leads to

$$\begin{aligned} q_s/q_{\text{ceiling}}(r=D) &= h_s/h_{\text{ceiling}}(r=D) \\ &= 3.5Re_H^{-0.12}(D/H)^{0.1}(D/H+0.279)/(D/H-0.0771); D/H \geq 0.2 \end{aligned} \quad (17)$$

where h_{ceiling} is the ceiling heat transfer coefficient.

"Typical" full-scale compartment fires with $(1-\lambda_r)Q$ in the range 200-2000kW and H in the range 2-3m are in the Re_H range $2(10^5)$ - $5(10^5)$, i.e., $Re_H^{-0.12} \approx 0.2$. The reduced-scale fires of [2-13] and [15] [$Q=0(1\text{kW})$, $H=0(1\text{m})$] were in the Re_H range $7(10^3)$ - $2(10^4)$, i.e., $Re_H^{-0.12} \approx 0.3$. For identical D/H , Eq.(17) therefore predicts that the magnitude of heat transfer amplification near the stagnation point is approximately 1.5 greater in the reduced-scale compartment fires than in a "typical" full-scale compartment fire. Results of Eq.(17) are plotted in Figure 5 for the two classes of fire. As can be seen, the results predict that in the "typical" full-scale fire, heat transfer amplification, i.e., $q_s/q_{\text{ceiling}}(r=D) > 1$, will only occur for D/H 's less than 1-1.5, while for the reduced-scale fires, amplification by a factor of 1.4 or greater will always occur in the small to moderate D/H range of interest.

7. COMPARISON WITH EXPERIMENTAL DATA

An experiment was carried out with a convective buoyant plume of strength $Q=0.117\text{kW}$ whose source was centrally located $H=1.22\text{m}$ below the ceiling of a tightly sealed, rectangular-plan enclosure ($2.13\text{m}\times 2.44\text{m}$) with controlled leakage from below [16]. For the experiment, $Q^*=0.657(10^{-4})$ and $Re_H=0.123(10^5)$. Data acquired included time-temperature measurements of the insulated, $0.79(10^{-3})\text{m}$ thick, galvanized steel walls and ceiling on a line from the plume impingement point and normal to the $D=1.22\text{m}$ ceiling-wall junction. Data near this junction led to the estimated experimental fluxes $q_s=8.0\text{W/m}^2$, $q_{\text{ceiling}}(r=D)=4.0\text{W/m}^2$. This is to be compared to the Eqs.(15)-(17) theoretical estimates $q_s=6.46\text{W/m}^2$ and $q_{\text{ceiling}}(r=D)=4.04\text{W/m}^2$, respectively. While these preliminary comparison are favorable, it is evident that more data, especially from stronger Q^* , Re_H buoyant sources, are required to validate the utility of the Eqs. (15)-(17) results of this paper.

8. OTHER USEFUL PROPERTIES OF THE CEILING JET

A determination of M_o' per Eq. (14) was key to an estimate of the ceiling jet stagnation heat transfer. M_o' will also be useful for future reference in characterizing the initial properties of the ceiling jet-driven wall flows of Figure 1, e. g., for use in applying the results of [6]. The ceiling jet mass flux per unit width, m_o' , and enthalpy flux per unit width, H_o' would also be useful in this regard. These are defined by

$$\dot{m}_0' = \rho v_{\max} \delta \int_0^{\infty} (v/v_{\max}) d(Z/\delta) \quad (18)$$

$$\dot{H}_0' = \rho C_p T_{\text{amb}} v_{\max} \delta \int_0^{\infty} (v/v_{\max}) (T/T_{\text{amb}} - 1) d(Z/\delta) \quad (19)$$

where T is the temperature in the ceiling jet, and where the above integrals can be estimated with use of

$$v/v_{\max} = \exp[-\ln(2) (Z/\delta)^2] \quad (20)$$

Using Eqs. (11)-(12) and (20) in Eq. (18) leads to

$$\dot{m}_0' / (\rho H v) = 0.088 (D/H)^{-0.2} \quad (21)$$

Beside depending on $\lambda_r Q$, the T distribution on which \dot{H}_0' is dependent will vary during the course of a given fire according to the heat transfer losses from the ceiling jet between $r=0$ and $r=D$. This can be estimated with use of

$$q_{\text{ceiling}} = h_{\text{ceiling}} (T_{\text{ad}} - T_{\text{ceiling}}) \quad (22)$$

where T_{ceiling} is the local ceiling surface temperature, and where h_{ceiling} and T_{ad} can be estimated from Eq. (6) of [5] and Eq.(16), respectively. Assuming the ceiling jet to be thin enough and/or the jet gases to

be transparent enough as to not play a significant role in radiative transfer, bounds for H_o' are easy to estimate. Thus, from $r=0$ to D the total rate of heat transfer from the ceiling jet, Q_{loss} , and then H_o' can be obtained from

$$Q_{loss} = 2\pi \int_0^D q_{ceiling} r dr \quad (23)$$

$$H_o' = [(1 - \lambda_r)Q - Q_{loss}] / (2\pi D) \quad (24)$$

The maximum possible value for H_o' , $H_o'_{(max)}$, would be for ceilings which behaved in an approximately adiabatic manner, i.e., negligible conduction into the surface, with limiting low effective surface emissivity, and, therefore, with $T_{ceiling} \approx T_{ad}$. Under such conditions all enthalpy convected from the fire's combustion zone would reach the $r = D$ wall location with $Q_{loss} = 0$, and

$$H_o'_{(max)} = (1 - \lambda_r)Q / (2\pi D) \quad (25)$$

The minimum value for H_o' , $H_o'_{(min)}$, would be for a ceiling which, from the initiation of the fire, had not yet been heated to temperatures significantly above its initial T_{amb} temperature. Under such circumstances, Q_{loss} can be estimated from Eqs. (22) and (23). The result of the indicated integration leads to

$$H_o'_{(min)} = H_o'_{(max)} \{ 1 - Q_{loss} / [(1 - \lambda_r)Q] \} \quad (26)$$

where, for the applicable D/H range of interest

$$Q_{\text{loss}}/[(1-\lambda_r)Q] = 2\pi[0.513 \text{Re}_H^{-1/2}\text{Pr}^{-2/3} + \text{Re}_H^{-0.3}\text{Pr}^{-2/3} I(D/H)], \quad 0.2 < D/H \quad (27)$$

$$I(\eta) = 0.0533 + \int_{0.2}^{\eta} [(\xi - 0.0771)/(\xi + 0.279)][f(\xi)/\xi^{0.2}]d\xi \quad (28)$$

and f is given in Eq. (16). $I(\eta)$ has been computed, and is plotted in Figure 6. Also, taking $\text{Pr} = 0.7$,

$Q_{\text{loss}}/[(1-\lambda_r)Q]$ is plotted in Figure 7 for different values of Re_H . As can be seen, this figure indicates that for any D/H the relative rate of ceiling heat transfer is significantly larger in reduced scale fires than in "typical" full scale fires.

9. AN ESTIMATE OF THE RANGE OF UTILITY OF THE RESULTS

The results developed here are based on the analogy drawn between free jet and buoyant plume-driven ceiling flows. While the analogy is strong for ceiling jet flow locations where Ri , the ratio of buoyancy to inertial forces, is small, the analogy and corresponding results are unreliable for moderate-to-large Ri . Such regions of unreliability can be established from an estimate of $\text{Ri}(D/H)$. Ri can be defined and obtained with the use of a characteristic temperature, T_{ch} , of the ceiling jet. This is taken here to be

$$\Delta T_{\text{ch}} = T_{\text{ch}} - T_{\text{amb}} = H_o'/(C_p m_o') \quad (29)$$

and Ri is defined as

$$Ri = g (\Delta T_{ch}/T_{amb}) \delta / v_{max}^2 \quad (30)$$

Using Eqs. (11), (12), (21), (25) and (29) in Eq. (30) leads to

$$Ri = Ri_{max} \{1 - Q_{loss}/[(1 - \lambda_r)Q]\} \quad (31)$$

$$Ri_{max} = 1.6(D/H)^{2.3}/(2\pi) \quad (32)$$

where Ri_{max} is the maximum possible value for Ri , corresponding to the adiabatic ceiling, i. e., $Q_{loss} = 0$.

The upper abscissa of Figure 7 is presented in units of Ri_{max} . Based on the above observations it is therefore evident from this figure that in the approximate range D/H of 2.-5. and larger, corresponding to Ri_{max} of 2.-10. and larger, the reliability of the Q_{loss} results, and, indeed, of all the results of this work must be brought into question on theoretical grounds. Finally, even for smaller D/H , experimental validation is required before the results presented here can be applied with confidence.

10. REFERENCES

- [1] Cooper, L.Y., Thermal Response of Unconfined Ceilings Above Growing Fires and the Importance of Convective Heat Transfer, 22nd Nat'l Heat Trans Conf, ASME paper 84-HT-105(1984).
- [2] Cooper, L.Y., Harkleroad, M., Quintiere, J., and Rinkinen, W., An Experimental Study of Upper Hot Layer Stratification in Full-Scale Multiroom Fire Scenarios, J Heat Trans, 104, p741(1982).
- [3] Cooper, L.Y., Convective Heat Transfer to Ceilings Above Enclosure Fires, 19th Symp (Inter) on Combustion, p933(1982).
- [4] Cooper, L.Y., Heat Transfer from a Buoyant Plume to an Unconfined Ceiling, J Heat Trans, 104, p446(1982).
- [5] Cooper, L.Y. and Woodhouse, A., The Bouyant Plume-Driven Adiabatic Ceiling Temperature Revisited, 23rd Nat'l Heat Trans Conf, ASME HTD-Vol45, p167(1985), to appear in J. Heat Trans.
- [6] Jaluria, Y. and Goldman, D., An Experimental Study of Negatively Buoyant Flows Generated in Enclosure Fires, Rutgers Univ, Nat'l Bur Stand (US) NBS-GCR-85-487(1985).
- [7] Alpert, R.L., Turbulent Ceiling-Jet Induced by Large-Scale Fires, Comb Sci and Tech, 11, p197(1975).

- [8] Poreh, M., Tsuei, Y.G., and Cermak, J.E., investigation of a Turbulent Radial Wall Jet, J Appl Mech, p457(1957).
- [9] Glauret, M.B., The Wall Jet, J Fl Mech, 1, p.625(1956).
- [10] Gardon, R. and Akfirat, J.C., Heat Transfer Characteristics of Impinging Two-Dimensional Air Jets, J Heat Trans, p101(1966).
- [11] Abramovich, G.N., The Theory of Turbulent Jets, MIT Press, p75(1963).
- [12] Yeldman, C.C., Kubota, T. and Zukoski, E.E., An Experimental Investigation of the Heat Transfer from a Buoyant Gas Plume to a Horizontal Ceiling - Part 1. Unobstructed Ceiling, Cal Inst Tech, Nat'l Bur Stand (US) NBS-GCR-77-97 (1975).
- [13] Zukoski, E.E. and Kubota, T., An Experimental Investigation of the Heat Transfer from a Buoyant Gas Plume to a Horizontal Ceiling - Part 2. Effects of Ceiling Layer, Cal Inst Tech, Nat'l Bur Stand (US) NBS-GCR-77-98 (1975).
- [14] Hegge Zijnen, B.G., Measurements of the Velocity Distribution in a Plane Turbulent Jet of Air, Appl Sci Res, A, 7, p256(1958).
- [15] You, H-Z. and Faeth, G.M., Ceiling Heat Transfer During Fire Plume and Fire Impingement, Fire and Materials, 103, p140(1979).
- [16] Mulholland, G., National Bureau of Standards, private communication.

11. NOMENCLATURE

B	Nozzle width
C_p	Specific heat at constant pressure
D	Wall-to-fire distance
f	Function in Eq. (16)
g	Acceleration of gravity
H	Ceiling-to-fire distance
H_o'	Enthalpy flux per unit width, Eq. (19)
$H_o'_{(max)}, H_o'_{(min)}$	Max, min possible values of H_o'
h	Heat transfer coefficient, Eq. (5)
h	Characteristic heat transfer coefficient
$h_s, h_{ceiling}$	h at wall stagnation, ceiling
I	An integral, Eq. (28)
k	Thermal conductivity
M_o'	Momentum flux per unit width, Eq. (1)
m_o'	Mass flux per unit width, Eq. (18)
Nu_o, Nu_s	Nusselt numbers., Eqs. (2) and (4)
Pr	Prandtl number
Q	Fire's energy release rate
Q_{loss}	Rate of heat loss to ceiling, Eq. (23)
Q^*	Dimensionless Q , Eq. (11)

q, q_{ceiling}	Convective heat transfer rate to wall, ceiling
q_s	q near wall stagnation
Re_e, Re_s, Re_H	Reynold's numbers, Eqs. (2), (4), and (5)
Ri	Richardson number, Eq. (30)
Ri_{max}	Maximum possible Ri
r	Distance from fire
T	Temperature in ceiling jet
T_{ch}	Characteristic T
T_{ceiling}	T at ceiling surface
$T_{\text{up}}, T_{\text{amb}}, T_w, T_{\text{ad}}$	Upper layer, ambient, wall, and adiabatic temperatures
V	Plane or ceiling jet velocity
V_e	Nozzle exit velocity
V_{max}	Maximum of V
V	Characteristic velocity, Eq. (11)
X	Distance from jet's virtual origin
X_n	Distance from nozzle
Z	Distance below ceiling
α, β	Constants, Eqs. (6)–(8)
ΔT_{ch}	Eq. (29)
δ	Z where $V/V_{\text{max}} = 1/2$

λ_r Fraction of Q radiated from combustion zone

μ Viscosity

ρ Density

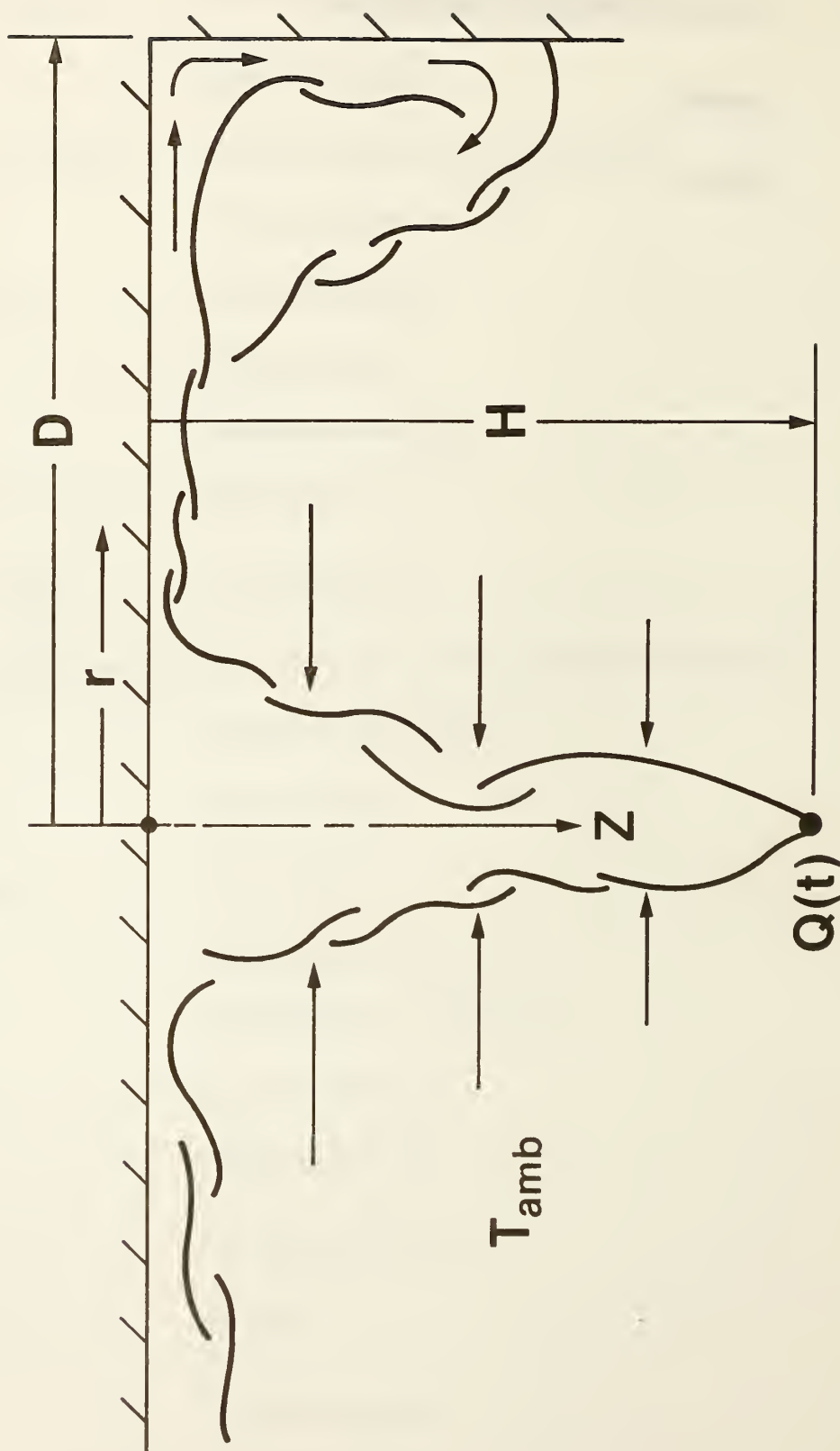
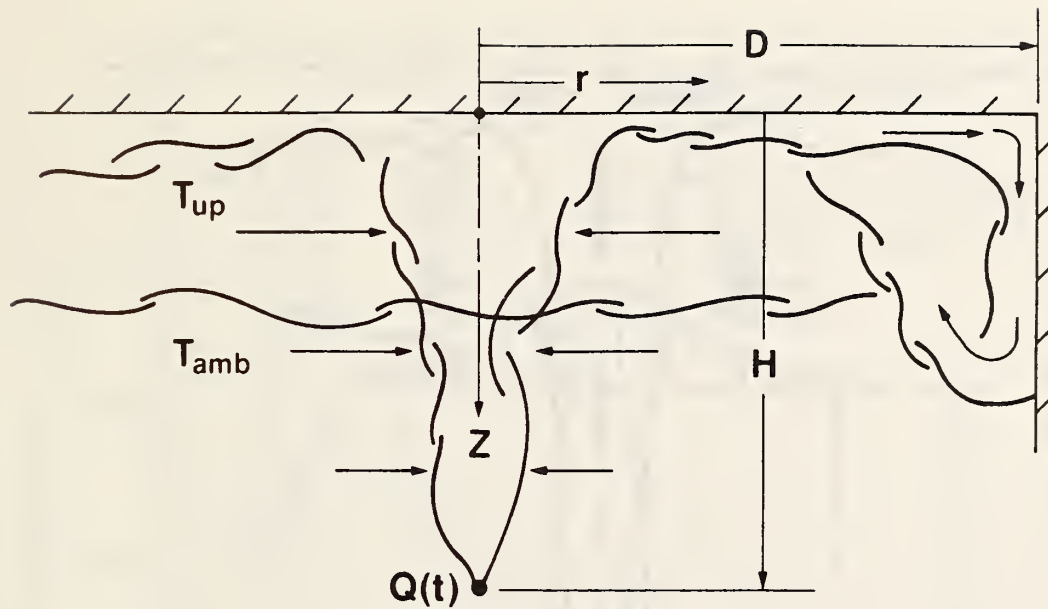
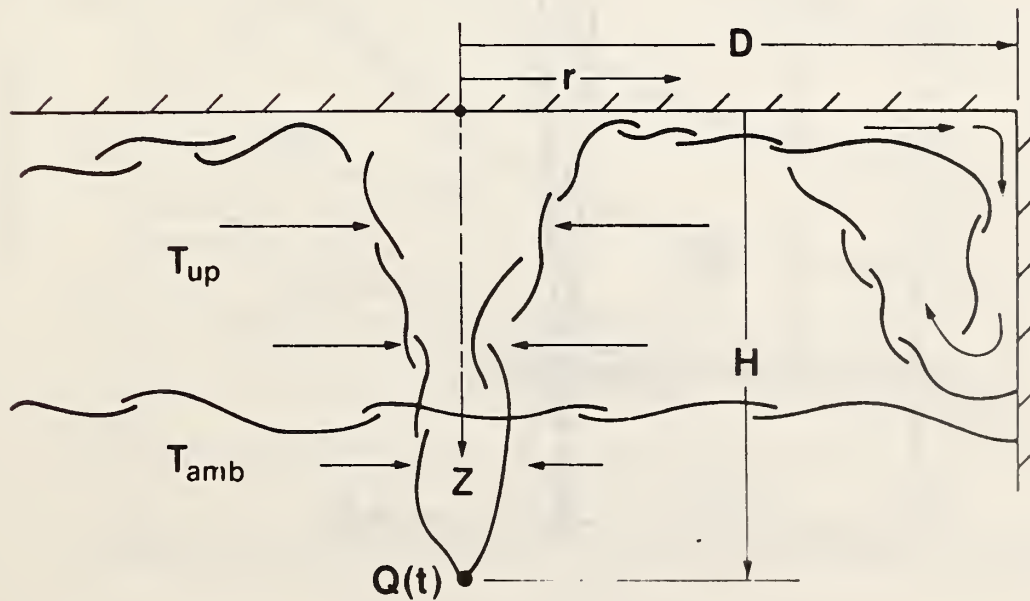


Figure 1 Early time ceiling jet-wall interaction.



a) penetration of interface



b) no penetration of interface

Figure 2. Ceiling jet-wall interaction with upper layer.

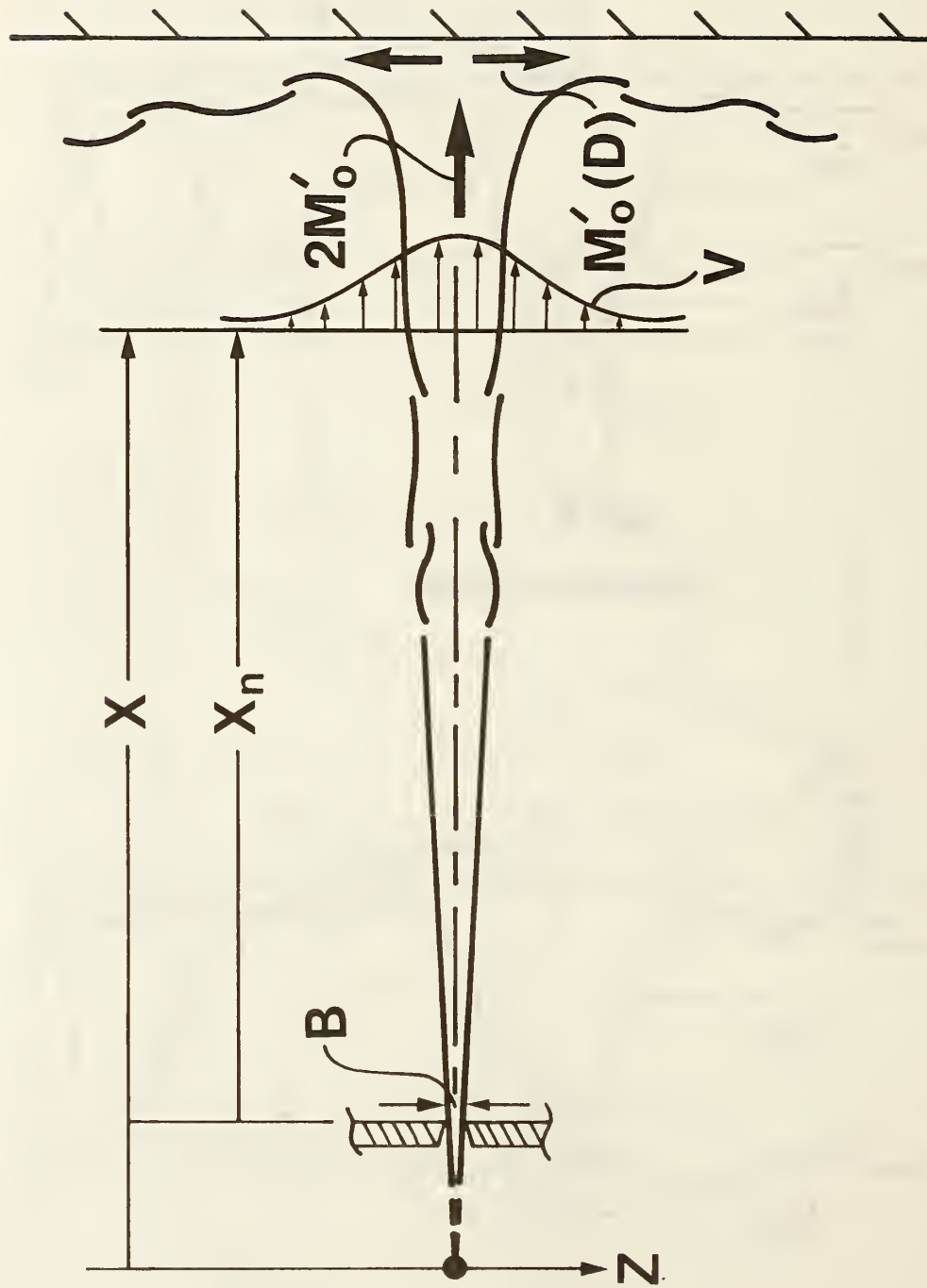


Figure 3 Plane jet-wall impingement.

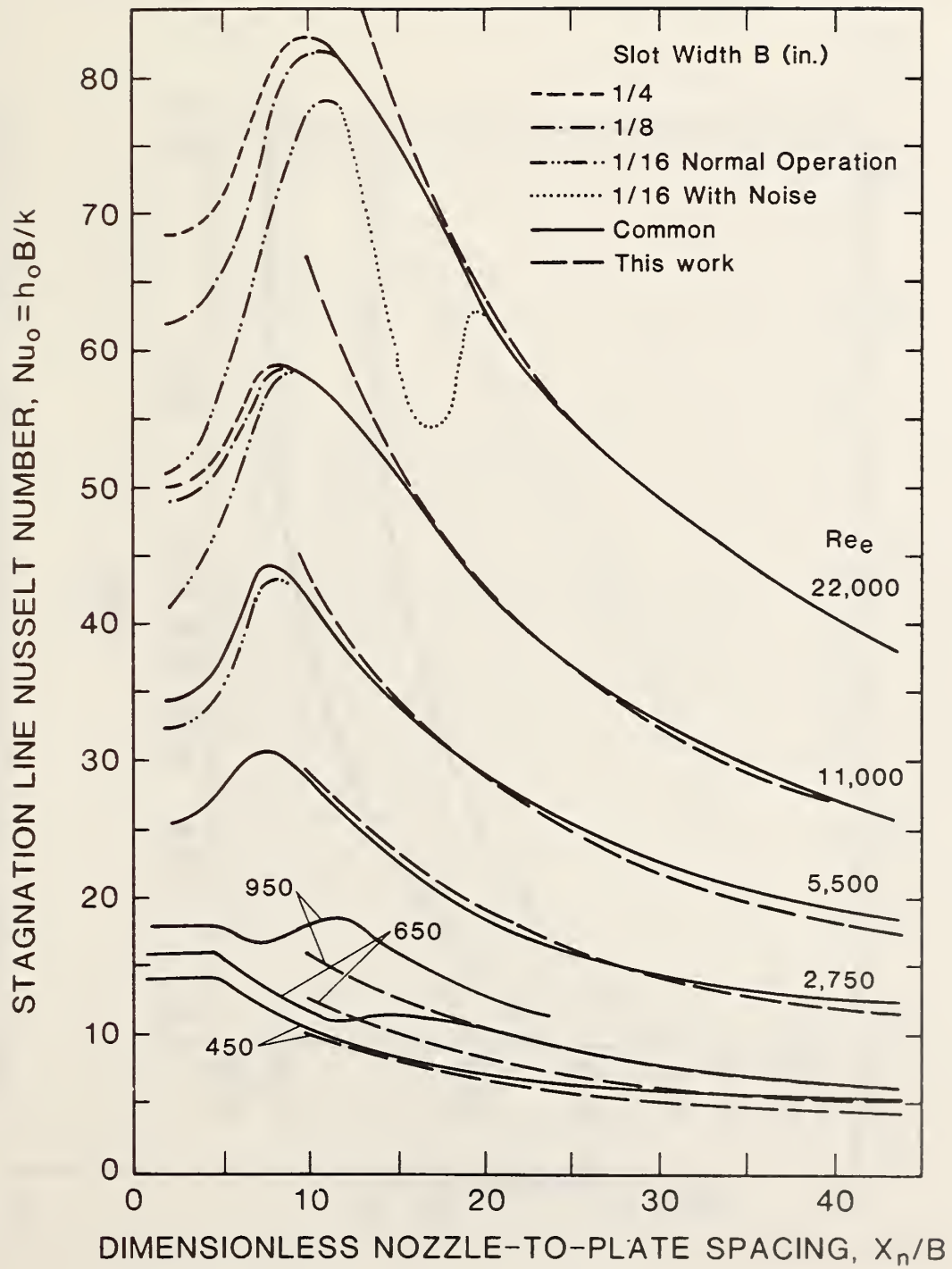


Figure 4. A plot of stagnation line Nusselt number from Figure 2 of [10] and from Eq (4).

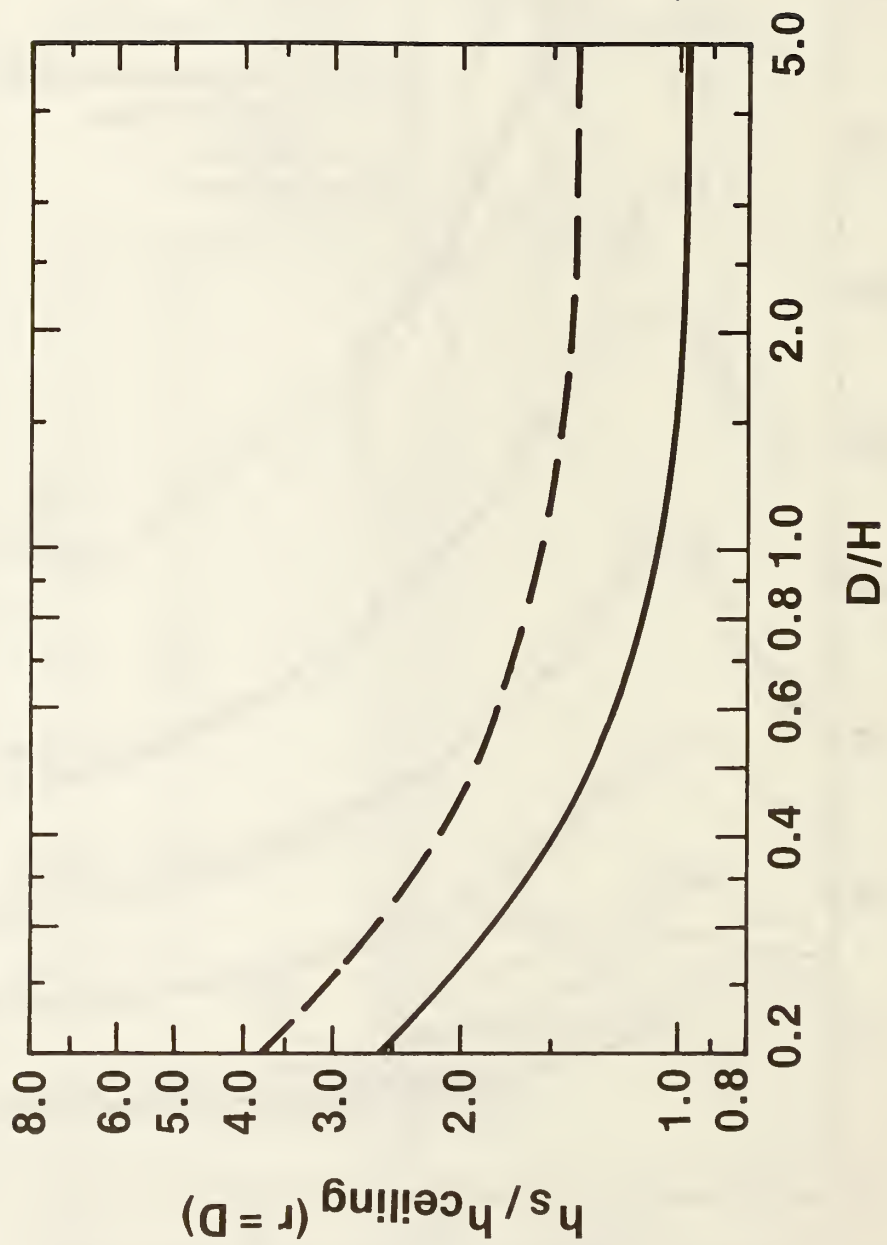


Figure 5. Stagnation point heat transfer amplification from Eq. (9): — "typical" full-scale; --- reduced scale.

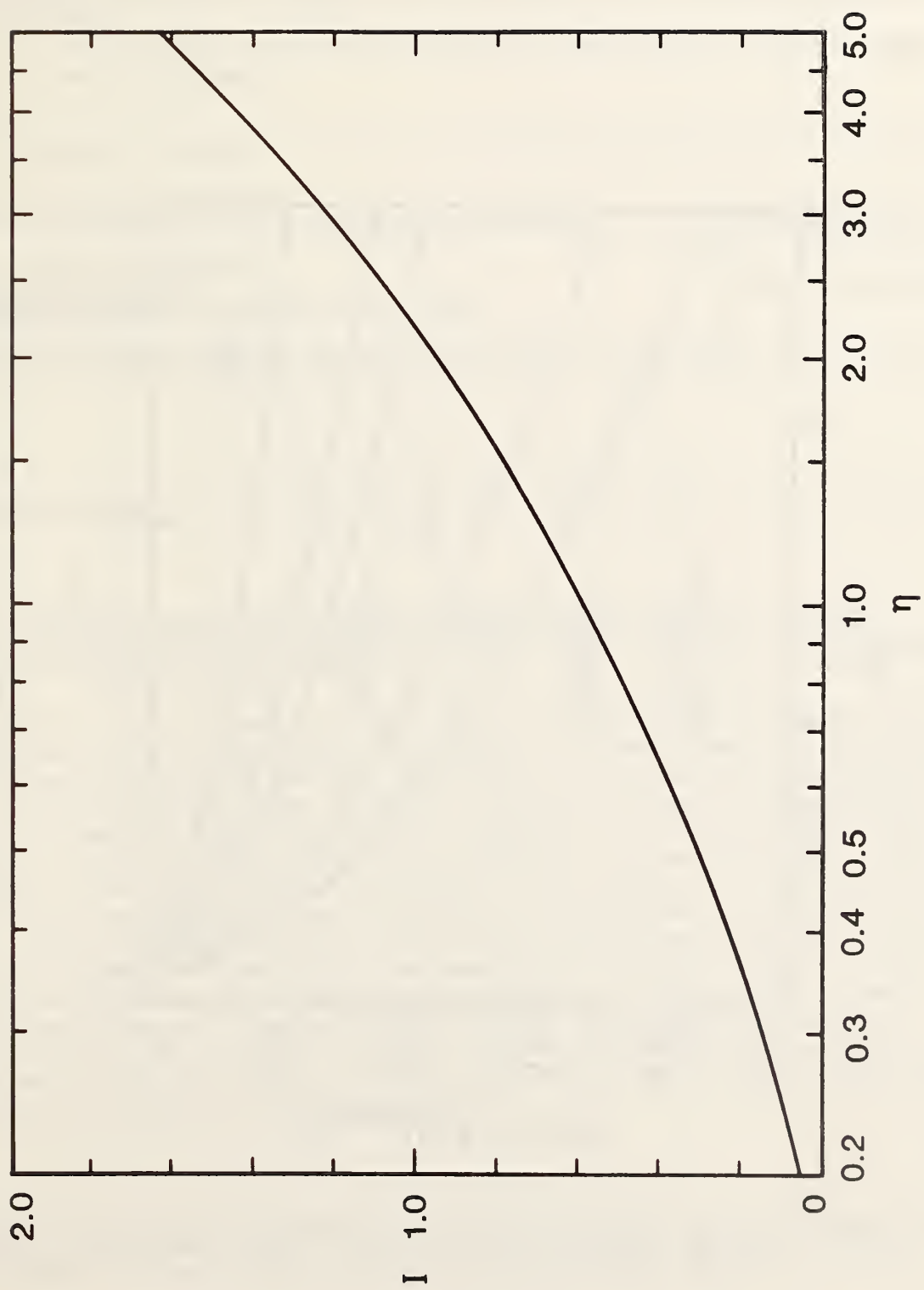


Figure 6. A plot of the integral I defined in Eq. (28).

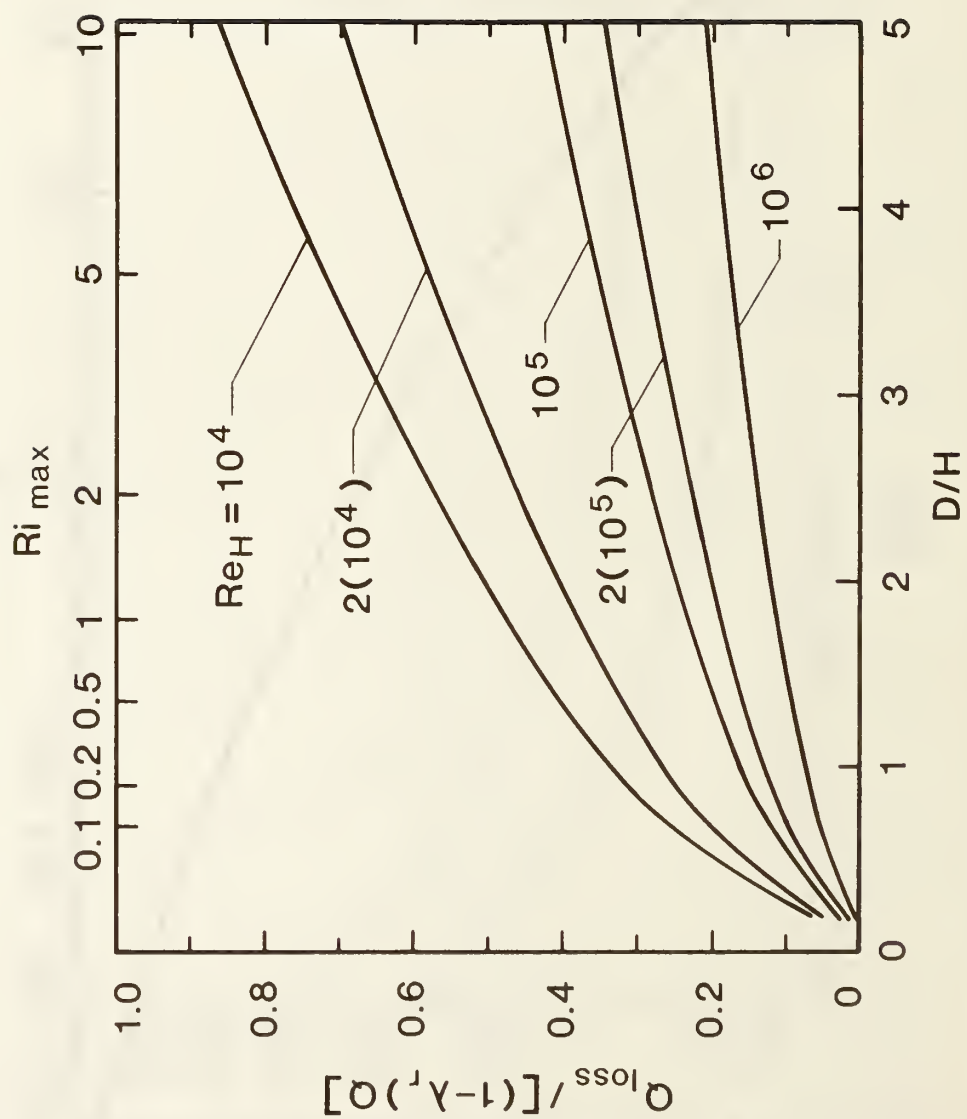


Figure 7. A plot of $Q_{\text{loss}} / [(1 - \lambda_r) Q]$ per Eqs. (27) and (32).

U.S. DEPT. OF COMM. BIBLIOGRAPHIC DATA SHEET (See instructions)		1. PUBLICATION OR REPORT NO. NBSIR-86/3307	2. Performing Organ. Report No.	3. Publication Date January 1986
4. TITLE AND SUBTITLE Ceiling Jet Properties and Wall Heat Transfer in Compartment Fire Near Regions of Ceiling Jet-Wall Impingement				
5. AUTHOR(S) Leonard Y. Cooper				
6. PERFORMING ORGANIZATION (If joint or other than NBS, see instructions) NATIONAL BUREAU OF STANDARDS DEPARTMENT OF COMMERCE WASHINGTON, D.C. 20234 Gaithersburg, MD 20899			7. Contract/Grant No.	
			8. Type of Report & Period Covered	
9. SPONSORING ORGANIZATION NAME AND COMPLETE ADDRESS (Street, City, State, ZIP)				
10. SUPPLEMENTARY NOTES				
<input type="checkbox"/> Document describes a computer program; SF-185, FIPS Software Summary, is attached.				
11. ABSTRACT (A 200-word or less factual summary of most significant information. If document includes a significant bibliography or literature survey, mention it here) The problem of heat transfer to walls from fire plume-driven ceiling jets during compartment fires is introduced. An analogy is drawn between the flow dynamics and heat transfer at ceiling jet-wall impingement and at the line impingement of a wall and a two-dimensional, plane, free jet. Using the analogy, the literature on plane, free jet flows and corresponding wall stagnation heat transfer rates leads to readily useable estimates for the heat transfer from, and the mass, momentum, and enthalpy fluxes of the turned compartment fire ceiling jet as it begins its initial descent as a negatively buoyant flow along the compartment walls. Available data from a reduced-scale experiment provides some limited verification of the heat transfer estimate. Depending on the proximity of a wall to the point of plume-ceiling impingement, the estimates indicate that for "typical" full-scale compartment fires with energy release rates in the range 200-2000kW and fire-to-ceiling distances of 2-3m, the rate of heat transfer to walls can be enhanced by a factor of 1-2.5 over the heat transfer to ceilings immediately upstream of ceiling jet-wall impingement.				
12. KEY WORDS (Six to twelve entries; alphabetical order; capitalize only proper names; and separate key words by semicolons) ceilings; compartment fires; convective heat transfer; enclosure fires; fire plumes; fire modeling; heat transfer; room fires; walls				
13. AVAILABILITY <input checked="" type="checkbox"/> Unlimited <input type="checkbox"/> For Official Distribution. Do Not Release to NTIS <input type="checkbox"/> Order From Superintendent of Documents, U.S. Government Printing Office, Washington, D.C. 20402. <input checked="" type="checkbox"/> Order From National Technical Information Service (NTIS), Springfield, VA. 22161			14. NO. OF PRINTED PAGES 33 15. Price \$9.95	

